

Purdue University
Purdue e-Pubs

ECE Technical Reports

Electrical and Computer Engineering

12-1-1992

The Impact of Adjustable Speed Drive Heat Pumps on Distribution Transformers

Kevin G. Karagory

Purdue University School of Electrical Engineering

Follow this and additional works at: <http://docs.lib.purdue.edu/ecetr>

Karagory, Kevin G., "The Impact of Adjustable Speed Drive Heat Pumps on Distribution Transformers" (1992). *ECE Technical Reports*. Paper 261.

<http://docs.lib.purdue.edu/ecetr/261>

This document has been made available through Purdue e-Pubs, a service of the Purdue University Libraries. Please contact epubs@purdue.edu for additional information.

THE IMPACT OF ADJUSTABLE SPEED DRIVE HEAT PUMPS ON DISTRIBUTION TRANSFORMERS

KEVIN G. KARAGORY

TR-EE 92-49
DECEMBER 1992



SCHOOL OF ELECTRICAL ENGINEERING
PURDUE UNIVERSITY
WEST LAFAYETTE, INDIANA 47907-1285

The Impact of
Adjustable Speed Drive Heat Pumps
on Distribution Transformers

Kevin G. Karagory

School of Electrical Engineering
Purdue University
Designated Professor: Prof. G.T. Heydt

TABLE OF CONTENTS

	Page
LIST OF FIGURES	iii
ABSTRACT	iv
CHAPTER 1 - INTRODUCTION	
1.1 Motivation and main objective	1
1.2 The adjustable speed drive heat pump	2
1.3 ANSI/IEEE Recommended Practice C57.110-1986	6
1.4 Literature summary	8
CHAPTER 2 - THE IMPACT OF THE ADJUSTABLE SPEED DRIVE HEAT PUMP ON THE DISTRIBUTION TRANSFORMER	
2.1 Simulation of the adjustable speed drive heat pump	10
2.2 Distribution transformer derating	27
2.3 Discussion	31
CHAPTER 3 - CONCLUSIONS AND RECOMMENDATIONS	
3.1 Conclusions	32
3.2 Recommendations for future work	32
LIST OF REFERENCES	34
APPENDIX	
PSpice Input File	36

LIST OF FIGURES

Figure	Page
1-1 Heat Pump in Heating Mode of Operation	3
1-2 Heat Pump in Cooling Mode of Operation	3
2-1 PSpice Circuit Model of the ASD Heat Pump System	11
2-2 Instantaneous Power Demand, Secondary Current.. and Secondary Voltage Waveforms for	
a. $\alpha = 0^\circ$	13
b. $a = 15^\circ$	14
c. $a = 30^\circ$	15
d. $\alpha = 45^\circ$	16
e. $\alpha = 60^\circ$	17
f. $\alpha = 75^\circ$	18
g. $a = 90^\circ$	19
2-3 Secondary Current Spectrum and Secondary Voltage Spectrum for	
a. $\alpha = 0^\circ$	20
b. $a = 15^\circ$	21
c. $\alpha = 30^\circ$	22
d. $a = 45^\circ$	23
e. $\alpha = 60^\circ$	24
f. $\alpha = 75^\circ$	25
g. $\alpha = 90^\circ$	26
2-4 Harmonic Spectrum of the Secondary Current	29
2-5 Total Harmonic Distortion in the Secondary Current	29
2-6 Harmonic Spectrum of the per unit Secondary Current	30
2-7 Distribution Transformer Capability	30

ABSTRACT

Electric utilities, by encouraging the use of high efficiency heat pumps, have increased the amount of power electronics in the residential sector. This report examines the impact that an adjustable speed drive heat pump **has** on the electric distribution transformer. Using a **PSpice** model of the components and ANSI/IEEE Recommended Standard C57.110-1986, the transformer capability to supply a nonsinusoidal load current to the residence is established.

CHAPTER 1

INTRODUCTION

1.1 Motivation and main objective

Every year brings major advances in the performance of power solid state devices. Lower prices are **concomitant** with these developments. Also, there has been continuing attention given to energy conservation and the associated benefits of **electric** power flow control. These factors have led to increasing use of power electronics in residential applications.

One of the first of these power devices to enter the consumer sector is the advanced generation heat pump. Although these devices encompass a wide variety of new types of **heat** pumps, this report focuses on models which employ an adjustable speed compressor. The continuously variable speed drive of the compressor offers substantially better energy efficiency.

The efficiencies realized by the introduction of high power electronics into heat pumps can also be directly applied to electric air conditioners. However, heat pumps have traditionally taken the lead in higher energy efficiencies. The results of this report can also be applied to the next generation of electric air conditioners.

The main objective of this report is to address the effect that residential high power electronics have upon the electric power distribution system. The specific application presented is the effect of adjustable speed drive (ASD) heat pumps on electric power distribution systems.

With the decreasing cost of power electronics comes an increasing use of such devices in the residential sector. **Many** electric utility companies have traditionally advocated increased energy efficiencies in household appliances as part of their demand-side management programs. They have done so with various types of credits **and/or** other financial benefit programs. The utilities have chosen this action for various reasons. Good public relations is one reason. Conservation of energy, and lowering consumers energy bills are other reasons for encouraging the use of high efficiency heat pumps. Their use may also improve the load factor for the electric utility. The electric utility company supports these programs under the belief that the high **efficiency** heat pumps have **no** negative impact on the distribution system. This report addresses this concern

1.2 The adjustable speed drive heat pump

The majority of heat pumps in residential applications are of the air-to-air type. [14]. Air is used both as the heat source and as the heat sink. The basic arrangements of heat pump components are shown in Figures 1-1 and 1-2 in both the heating and cooling modes of operation respectively. The heat pump consists of an evaporator, a condenser, two fans, an expansion device, a compressor, and a compressor drive. In most residential applications the vapor compression system is used for the refrigeration process [3]. Cool low-pressure liquid refrigerant enters the evaporator and evaporates. As it evaporates, it absorbs heat from the air

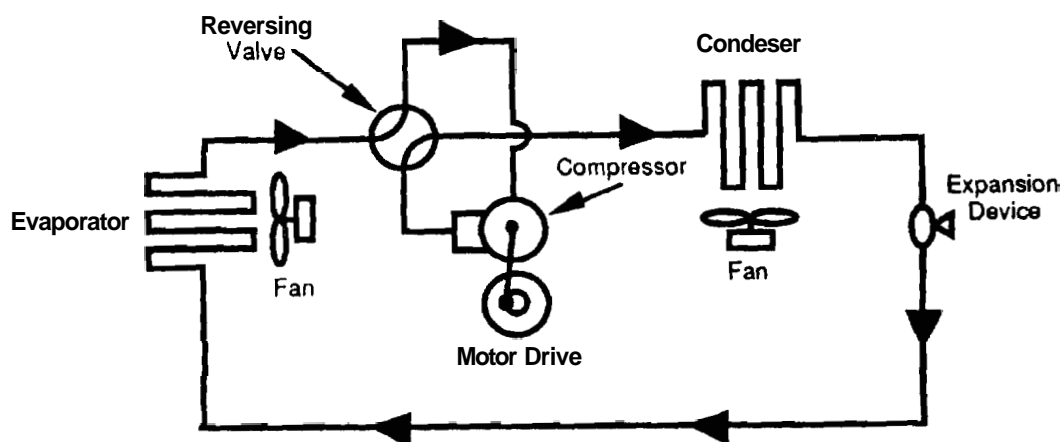


Figure 1-1
Heat Pump in **Heating** Mode of Operation

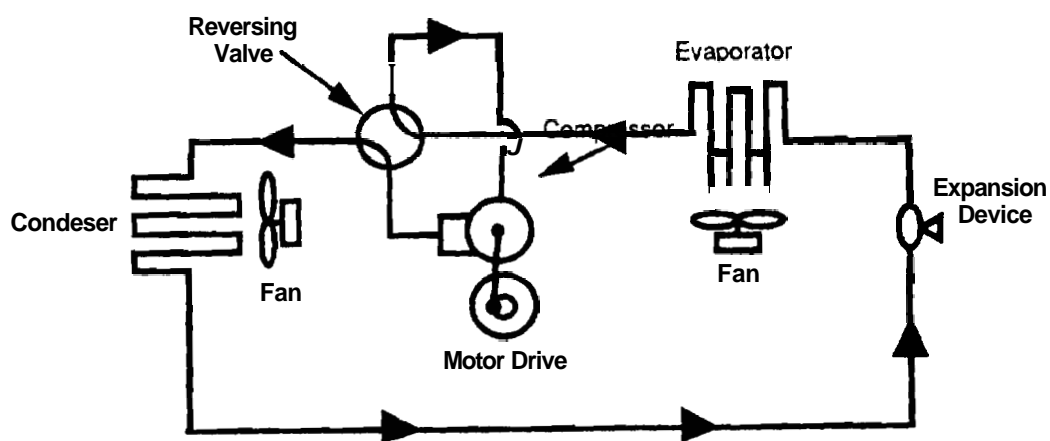


Figure 1-2
Heat Pump in **Cooling** Mode of Operation

surrounding the evaporator. The refrigerant then leaves the evaporator as a cool low-pressure gas. It then enters the compressor where its pressure and temperature are increased. The **refrigerant** is then discharged as a hot high-pressure gas to the condenser. There it condenses into a liquid and **releases** heat into the air. The temperature of the air surrounding the condenser is lower than that of the refrigerant gas. The hot high-pressure liquid then flows through the expansion valve back to the evaporator. The expansion valve reduces the hot high-pressure refrigerant liquid back to a cool low-pressure liquid. thus completing the cycle.

Conventional heat **pumps** must continually cycle "off" and "on" to maintain a comfortable indoor temperature, due to the fact that the compressor drive operates at only one speed. Thus, the heat pump must run at full capacity whenever it is operative. With the ASD heat pump the compressor speed can vary to closely match the **heating/cooling** load of the home. This leads to superior energy efficiency [3]. The indoor **temperature** can be kept within a much smaller tolerance, providing a greater comfort level. Better humidity control is also obtained with a system which is continually operative.

Similar economies are gained by the use of variable speed fans. This report does not address this concern. It is assumed the greater gains in energy efficiencies **are** had with the use of adjustable speed compressors. Thus, the fans on the condenser and evaporator being considered are single speed.

The higher energy efficiency is achieved by allowing the refrigerant the longest amount of time possible in the evaporator and

condenser while still meeting the load **requirement**. This leads to greater heat transfer in these two heat exchangers given the same amount of refrigerant passing through these components. Assuming the same amount of electrical energy is needed to circulate a given amount of refrigerant through the system, a net increase in heat transfer is accomplished. Thus, higher energy efficiency is achieved.

Reciprocating compressors are almost exclusively the type used in residential heat pumps today [14]. The scroll compressor is seen by some as the compressor which will eventually replace its reciprocating counterpart. The scroll compressor does offer higher efficiencies and presents a much smoother load torque to the compressor drive. However, this report only deals with the reciprocating compressor since it is the dominant type in residential heat pumps in use today.

The drives of residential heat pumps are typically two-pole, single-phase induction motors. These directly drive the compressors. Various exotic strategies exist for adjusting the speed of the electric motor drive. These variable-frequency converter types include the pulse-width-modulated voltage-source inverter, the square-wave voltage-source inverter, and the current-source inverter. The drive considered in this report is a variable-voltage, constant-frequency type. This **design** was chosen because of its simplicity. Back-to-back thyristors or a triac are connected in series with the stator. When the firing angle of the thyristors is delayed, a chopped sinusoid voltage is applied to the stator winding. Thus, the fundamental frequency component of the stator voltage is reduced by delaying the

firing angles of the thyristors. A variable speed drive is then achieved.

1.3 ANSI/IEEE Recommended Practice C57.110-1986

The IEEE recommended practice for establishing transformer capability when supplying non sinusoidal load currents is contained in an American National Standard ANSI/IEEE C57.110-1986. This is an extremely complicated subject and may require extensive computer analysis for an exact solution. This recommended practice presents approximate techniques for determining a conservative estimate of the capability of transformers to supply **non sinusoidal** load currents **without** loss of **normal** life expectancy.

Higher harmonic content in the load current increases the eddy current loss in the transformer. These increased eddy currents occur in all iron parts of the transformer. The increased eddy currents lead to a higher operating temperature of the transformer. This, in turn results in a shortened useful life of the transformer. There are also I^2R losses in the transformer winding, terminals, and other current carrying components. If I is larger due to harmonics, the I^2R losses will be correspondingly higher. The ANSI/IEEE Recommended Practice C57.110-1986 considers both loss types.

The application of this recommended practice is limited to **dry**-type distribution and power transformers, and liquid-immersed power transformers up to SOMVA rating, when subjected to non sinusoidal load currents which have a harmonic factor exceeding 0.05 per unit. Two methods are described in ANSI/IEEE C57.110-1986 for

determining the derating of the transformer. The first method assumes availability of information on the loss density distribution within the transformer windings. The second method assumes access to transformer certified test report data. This section discusses the first method. The latter method is less accurate and is primarily employed by users.

The transformer is presumed to be operating under usual service conditions other than its high load current harmonic factor. ANSI/IEEE C57.110-1986 establishes a current derating factor for load currents having a given harmonic composition. The transformer capability equivalent is given by

$$I_{MAX} = \sqrt{\frac{P_{LL}}{1 + \left(\frac{\sum_{h=1}^{h_{MAX}} f_h^2 h^2}{\sum_{h=1}^{h_{MAX}} f_h^2} \right) P_{EC}}} \quad (1-1)$$

The maximum permissible non sinusoidal load current with a given harmonic composition is given by I_{MAX} . The parameter P_{LL} is the load loss density under rated conditions expressed in per unit of rated I^2R loss density. The parameter P_{EC} is the winding eddy current loss under rated conditions expressed in per unit of rated I^2R loss density. The harmonic order is given by h . The harmonic current distribution factor for harmonic h is given by f_h , where f_h is I_h/I . This ratio is equal to the harmonic (h) component of the current divided by the fundamental (60Hz) component of the current. Equation 1-1 gives the maximum load current which will

ensure that the losses of the windings do not exceed the value of losses under **rated 60Hz** operating conditions.

1.4 Literature summary

The subject of this report falls into the category of electric power quality [1]. A particularly important area within electric power quality relates to **harmonic** voltages and currents in distribution systems. These harmonics result from nonlinear loads. Analysis of harmonics in the distribution system is readily accomplished using a numerical solution technique (**e.g., PSpice**) followed by calculation of the voltage and current spectrum (**e.g.,** using the fast Fourier **transform** or FFT). This method is covered in depth in [2].

A particularly **significant** source of harmonics in the residential sector is attributed to high efficiency heat pumps. The entire subject of heat pumps is analyzed in [3]. This includes a large discussion of the thermodynamic principles which are involved. The advanced generation heat pump referred to in this report is presented in references [4,5]. Strong motivation for implementing such devices is provided for electric utilities and consumers alike. The environmental benefits of adjustable speed drive applications is shown in an **EPRI** report of similar name [6].

The electronic drive **common** to heat pump applications is presented in [7]. Various adjustable speed drives are analyzed in [8]. Also discussed are harmonic compensation techniques. The electric motor model used in this report was taken from [9].

The modeling of the electric distribution system, electronic drive, and motor was done on Macintosh using PSpice by Microsim Corporation [10]. An excellent beginning book on circuit simulation using PSpice is given by [11]. Reference [12] provided a resource for advanced topics on SPICE.

CHAPTER 2

THE IMPACT OF THE ADJUSTABLE SPEED DRIVE HEAT PUMP ON THE DISTRIBUTION TRANSFORMER

2.1 Simulation of the adjustable speed drive heat pump

The PSpice circuit simulation used to represent the ASD heat pump, the distribution transformer, and the distribution system is shown in Figure 2-1. The corresponding PSpice input (circuit) file is given as the Appendix.

As shown in Figure 2-1, the system voltage is set by VIN to 220V RMS. The distribution system impedance is assumed to be purely reactive. The system impedance is represented by LSYS of 0.8mH. The distribution transformer is modeled by a series impedance given by RXFRM and LXFRM of 0.007Ω and 0.18mH, respectively.

In parallel with the ASD heat pump is a resistive element RLOAD of 75Ω . This is used to model other load currents at the residence. This non-ASD heat pump current is 2.9A RMS.

The variable-voltage, constant-frequency motor drive electronics are represented by the thyristors XSCR1 and XSCR2. The PSpice model of the thyristors can be examined in detail in the Appendix. The turn on time of the thyristors, given by a in degrees of the nominal system frequency of 60Hz, was allowed to be 0° , 15° , 30° , 45° , 60° , 75° and 90° in the circuit simulations.

The induction motor is represented by the equivalent circuit model consisting of L1, XRES, L2, R2, L3 and R3. The use of this

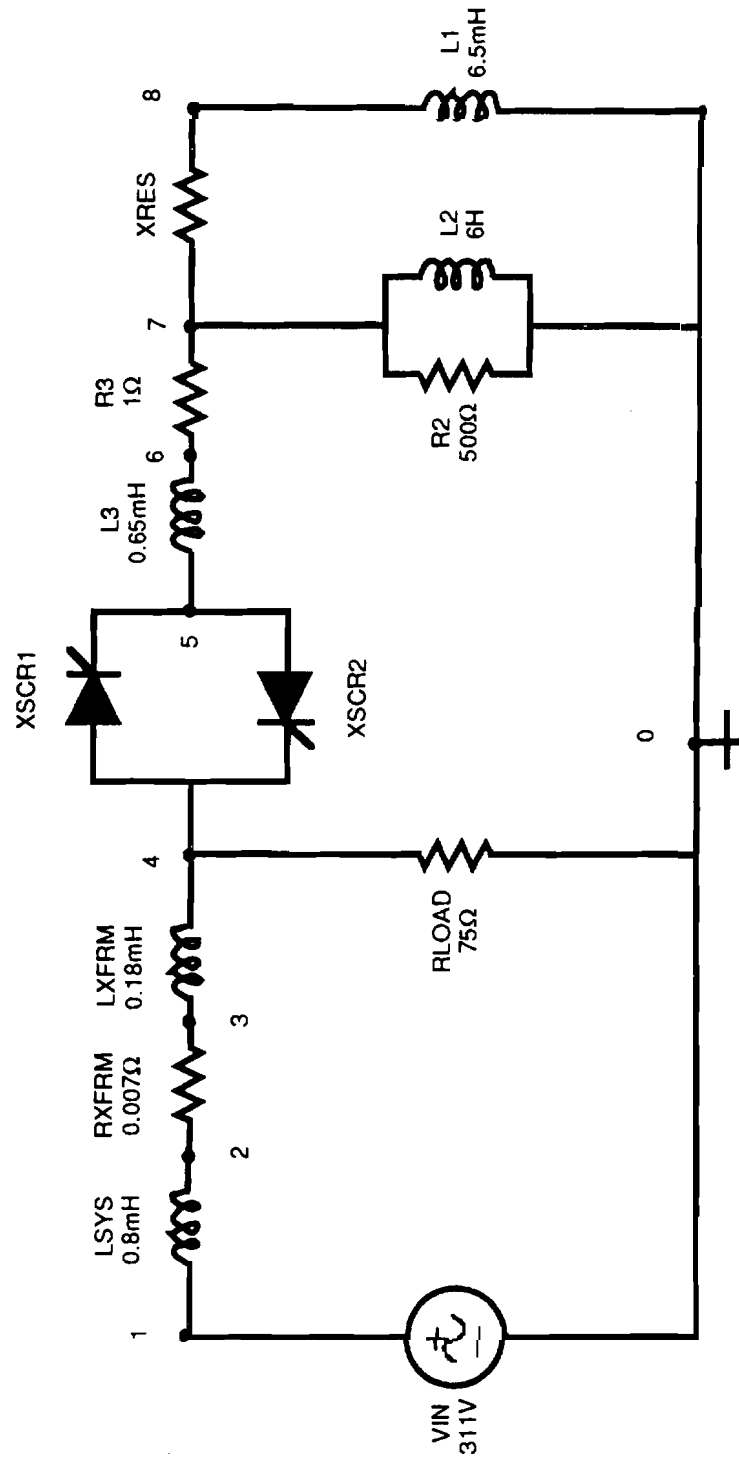


Figure 2-1
PSpice Circuit Model of the ASD Heat Pump System

simple model for the application is discussed in Section 2.3. The element XRES is a time varying resistor and is explained further in the next paragraph. The inductors L1, L2 and L3 have the values 6.5mH, 6H and 0.65 mH, respectively. The resistive elements are given by R2 of 500 Ω and R3 of 1 Ω as shown in Figure 2-1..

The PSpice circuit element XRES simulates a time varying resistor of the form given by Equation 2-1. The time is given by t . The frequency ω is the nominal system frequency of 120π rad/s. The slip of the induction motor is represented by SLIP and is 1/6 in the simulation. The expression for R_{XRES} is,

$$R_{XRES} = 10 + 4\sin(2\omega(1-SLIP)t) \Omega. \quad (2-1)$$

The resistance of this circuit element is allowed to vary in order to more accurately model the varying load torque produced by the ASD heat pump compressor. Since the compressor is directly coupled to the induction motor, the compressor rotational drive frequency ω_c is the same as the induction motor mechanical frequency, ω_m . Assuming a two-pole motor, ω_c equals $\omega(1-slip)$, where ω represents the nominal frequency of 120π rad/s for the system. The frequency ω is doubled to reflect both the compression and suction strokes of the compressor piston during one electrical cycle.

Each simulation was allowed to run for 50ms. The instantaneous power demand, secondary current, and secondary voltage waveforms for the various delay angles α are shown in Figure 2-2a through 2-2g. The fast Fourier transform of the secondary current and the secondary voltage for the various α are shown in Figures 2-3a through 2-3g.

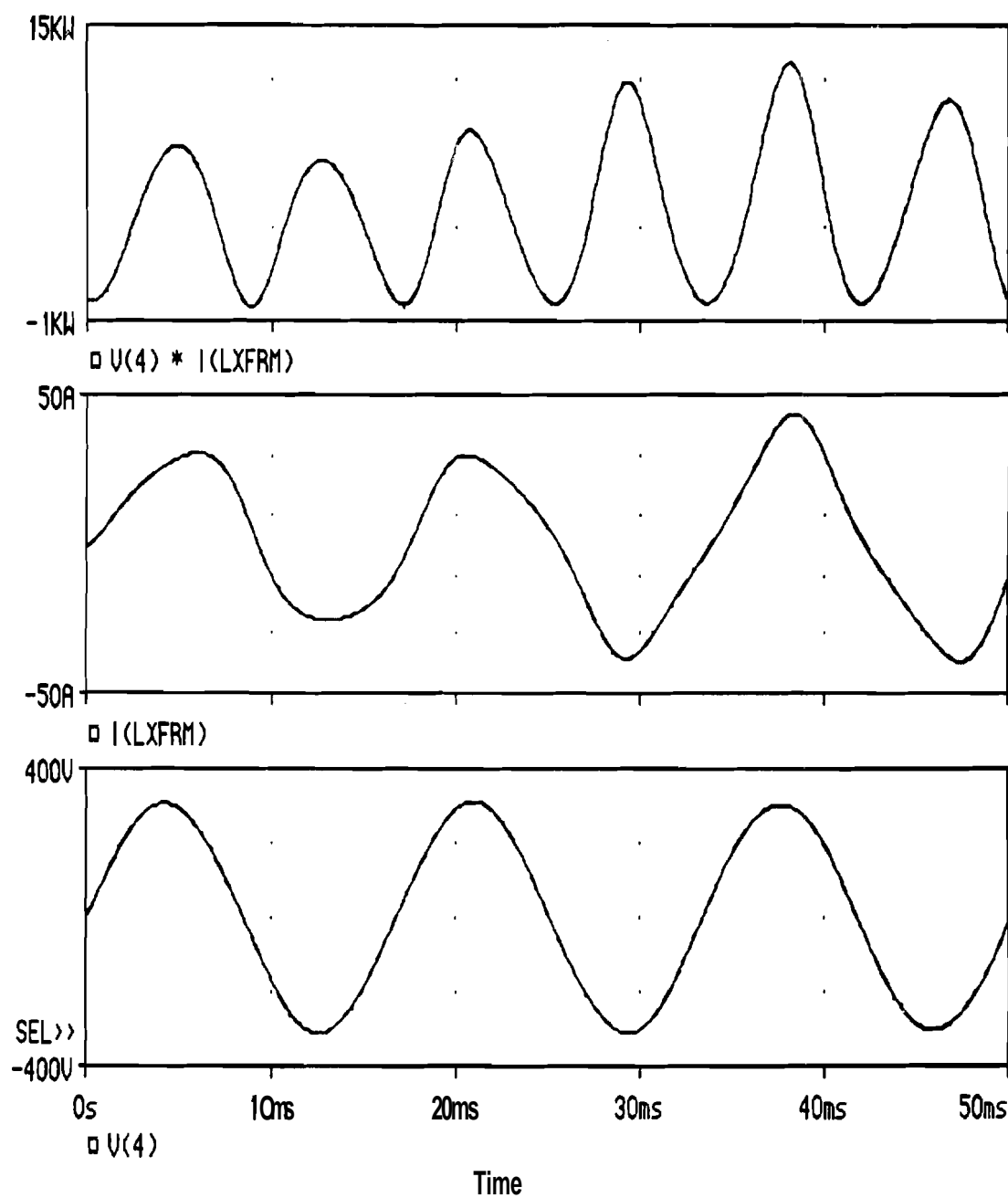


Figure 2-2a
 Instantaneous Power Demand,
 Secondary Current,
 and Secondary Voltage Waveforms
 for $\alpha = 0^\circ$

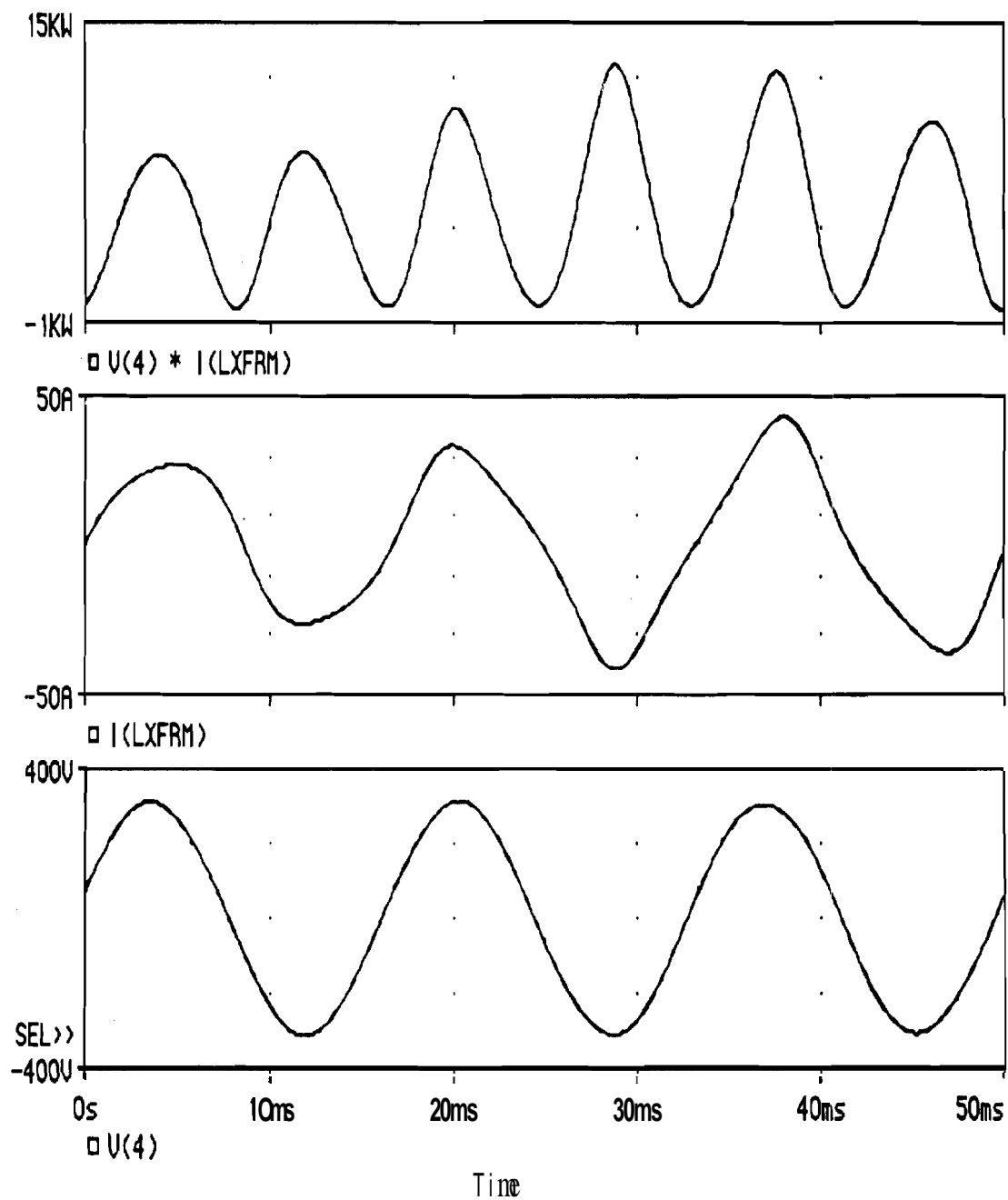


Figure 2-2b
 Instantaneous Power Demand,
 Secondary Current,
 and Secondary Voltage Waveforms
 for $\alpha = 15^\circ$

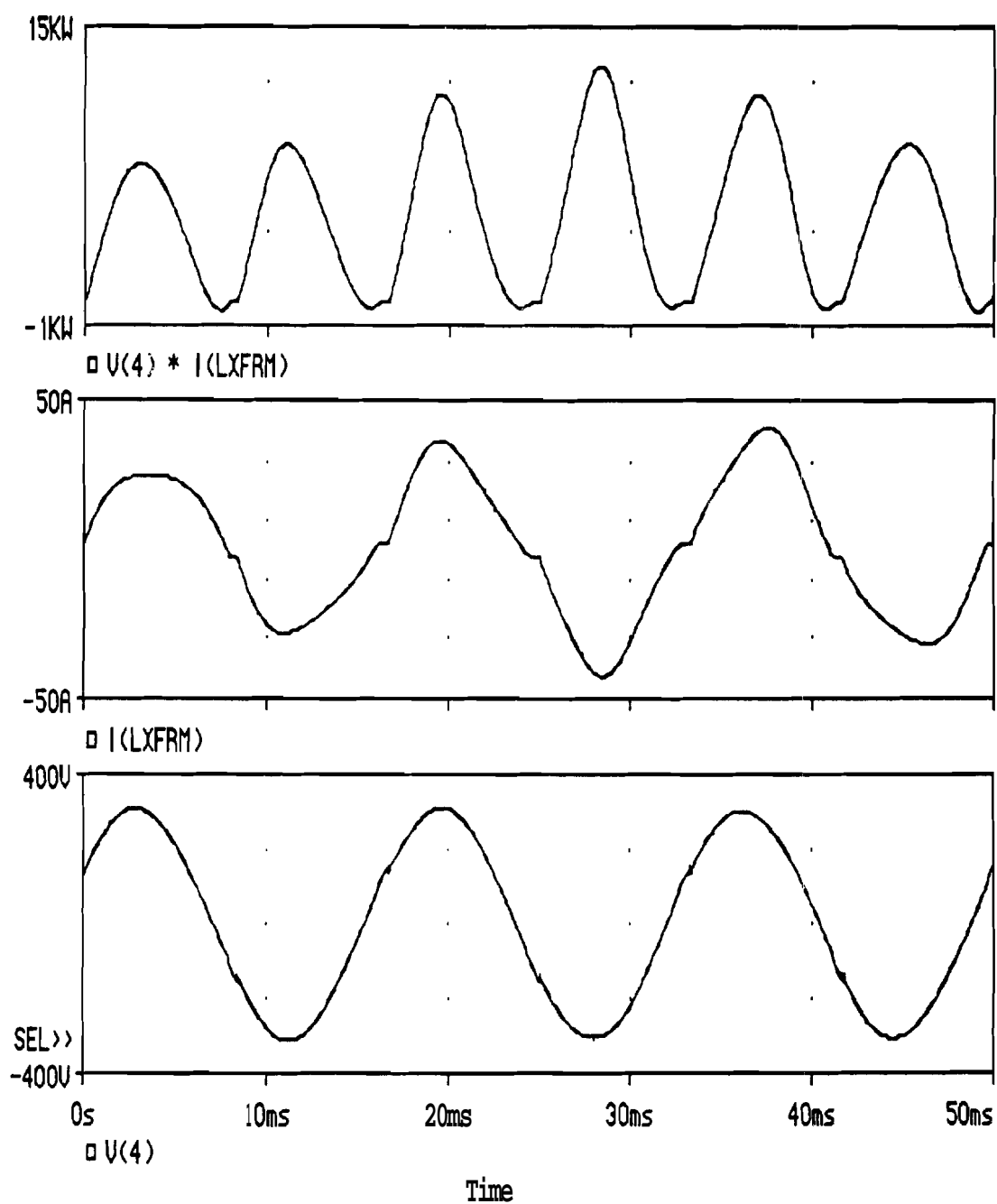


Figure 2-2c
 Instantaneous Power Demand,
 Secondary Current,
 and Secondary Voltage Waveforms
 for $\alpha = 30^\circ$

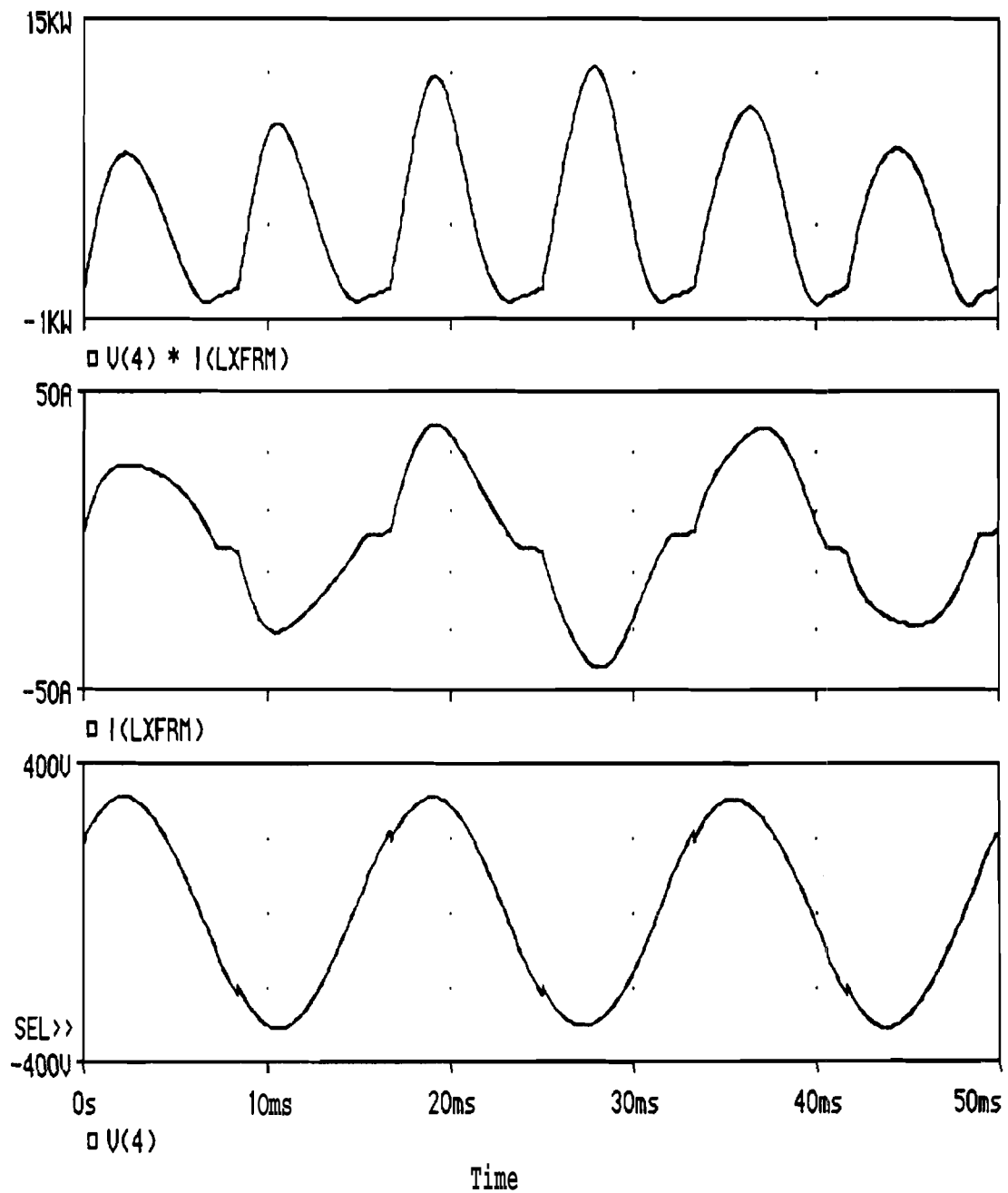


Figure 2-2d
 Instantaneous Power Demand,
 Secondary Current,
 and Secondary Voltage Waveforms
 for $\alpha = 45^\circ$

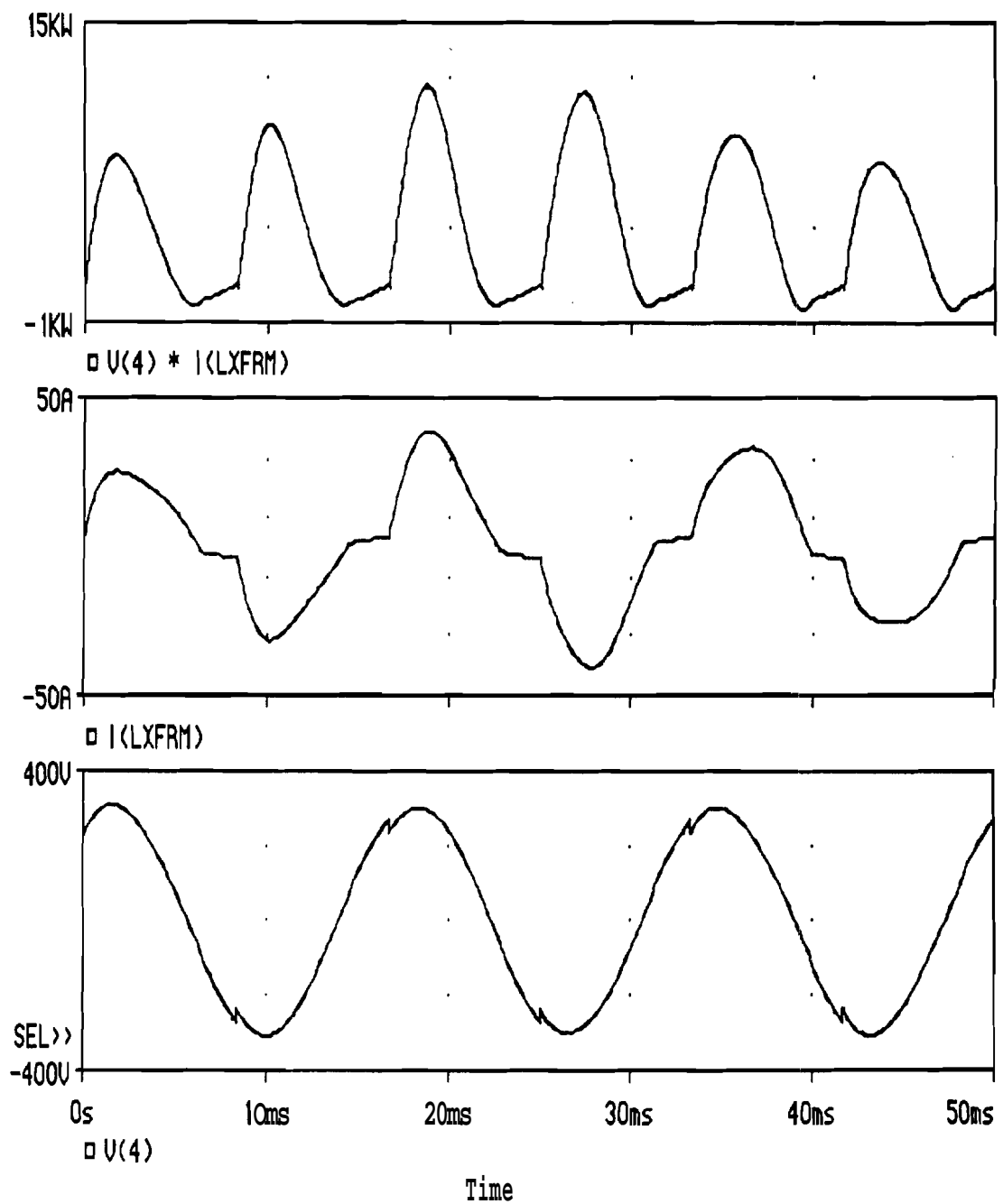


Figure 2-2e
Instantaneous Power Demand,
Secondary Current,
and Secondary Voltage Waveforms
for $\alpha = 60^\circ$

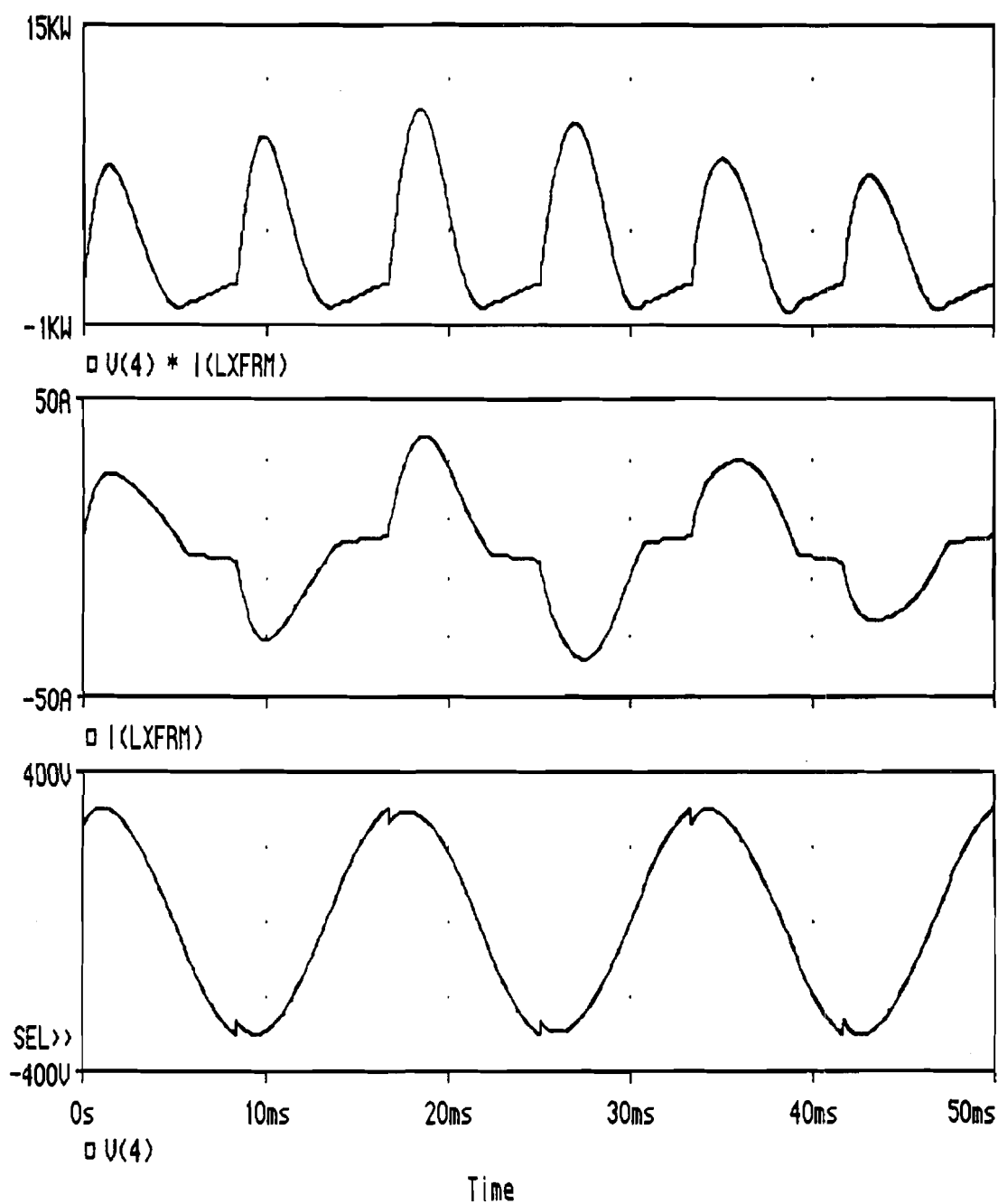


Figure 2-2f
Instantaneous Power Demand,
Secondary Current,
and Secondary Voltage Waveforms
for $\alpha = 75^\circ$

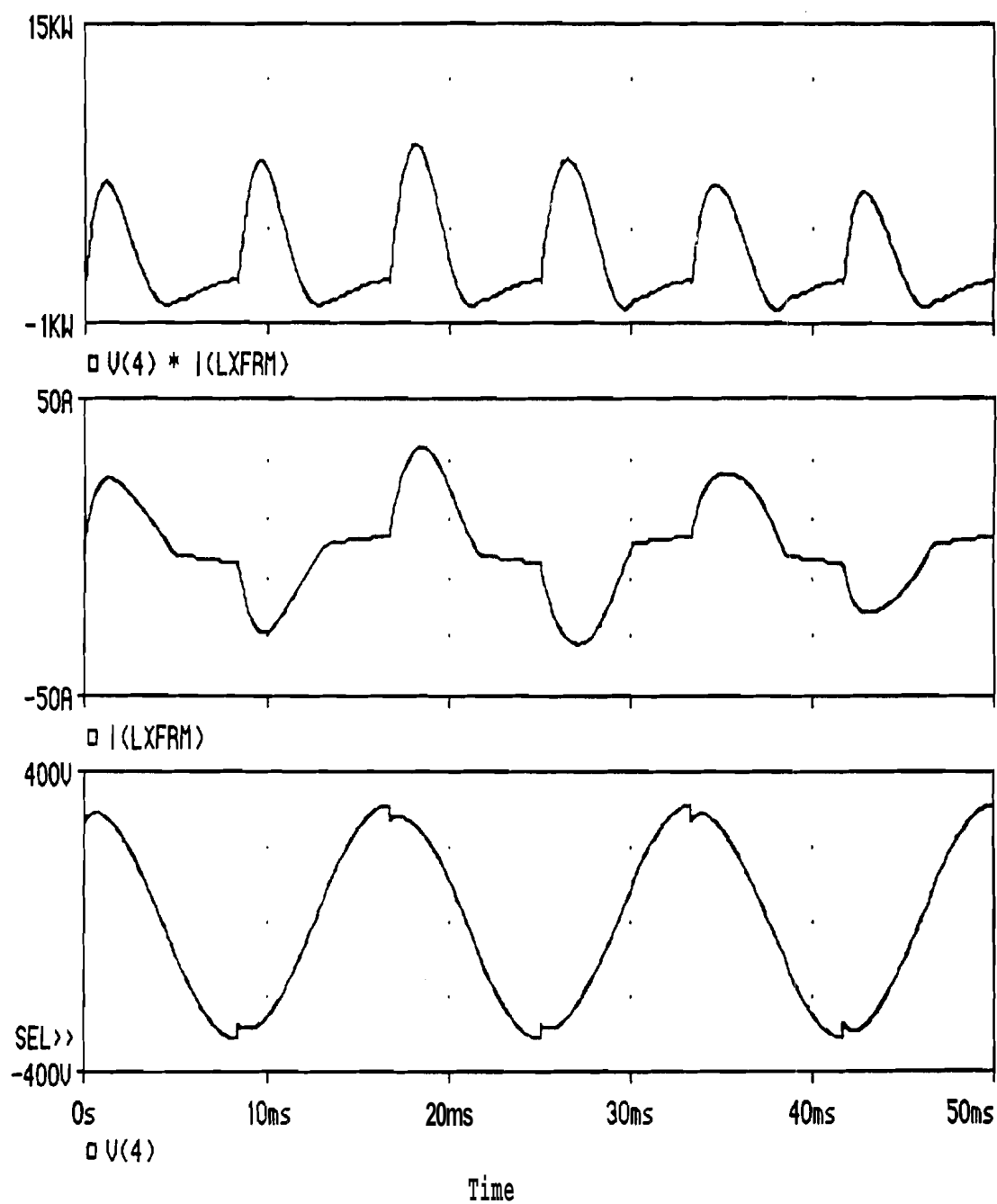


Figure 2-2g
 Instantaneous Power Demand,
 Secondary Current,
 and Secondary Voltage Waveforms
 for $\alpha = 90^\circ$

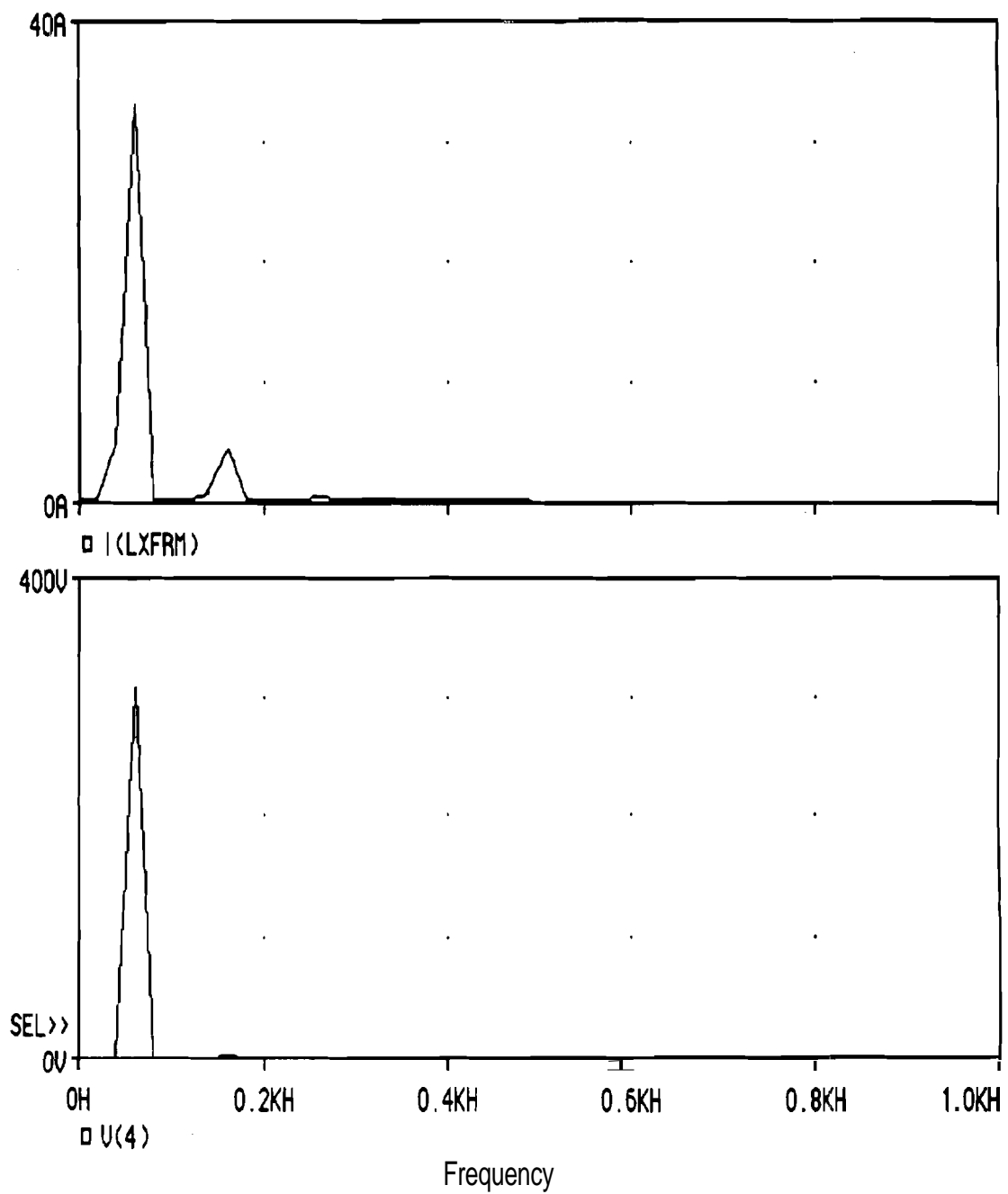


Figure 2-3a
Secondary Current Spectrum,
and Secondary Voltage Spectrum
for $\alpha = 0^\circ$

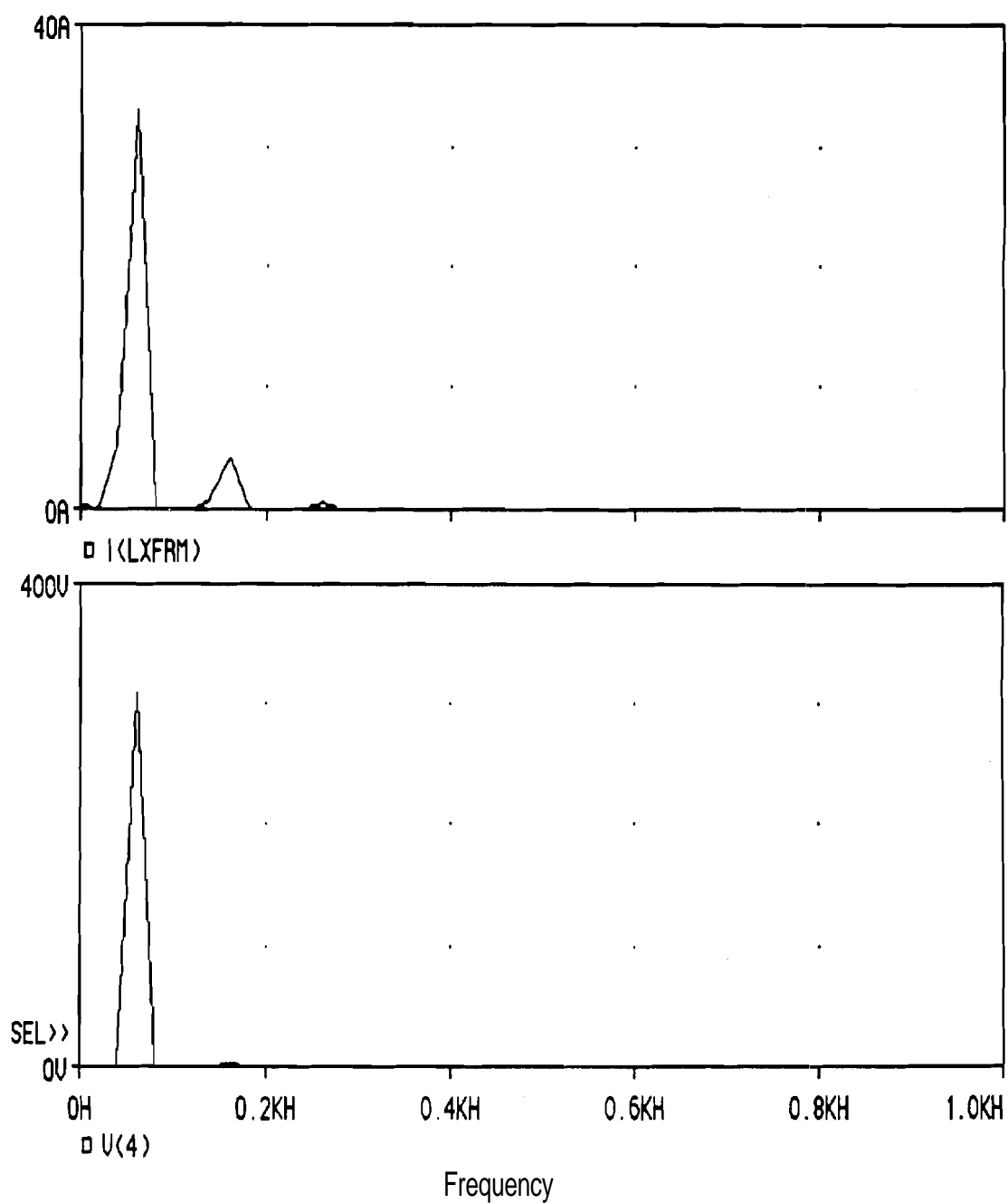


Figure 2-3b
 Secondary Current Spectrum,
 and Secondary Voltage Spectrum
 for $\alpha = 15^\circ$

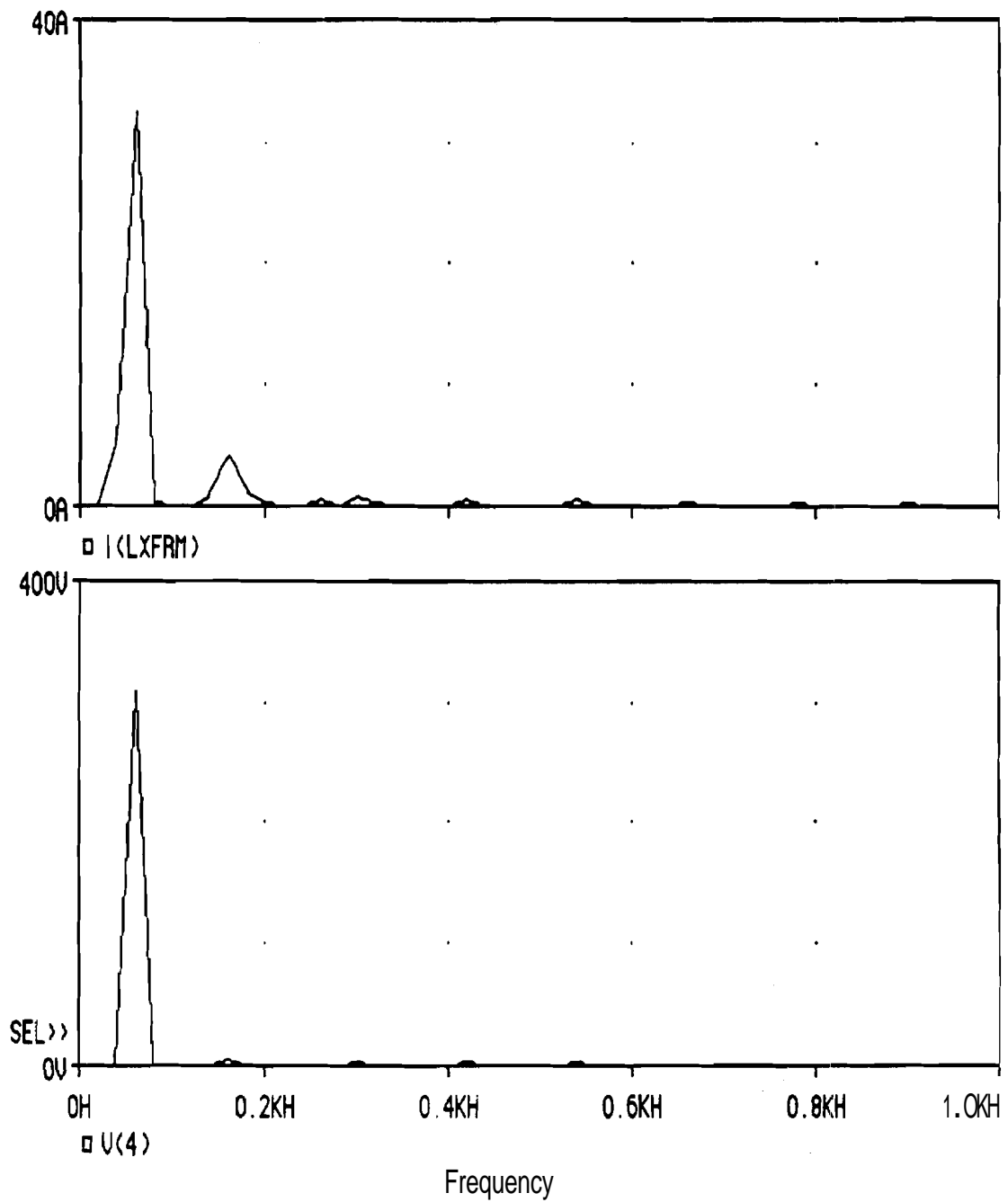


Figure 2-3c
 Secondary Current Spectrum,
 and Secondary Voltage Spectrum
 for $\alpha = 30^\circ$

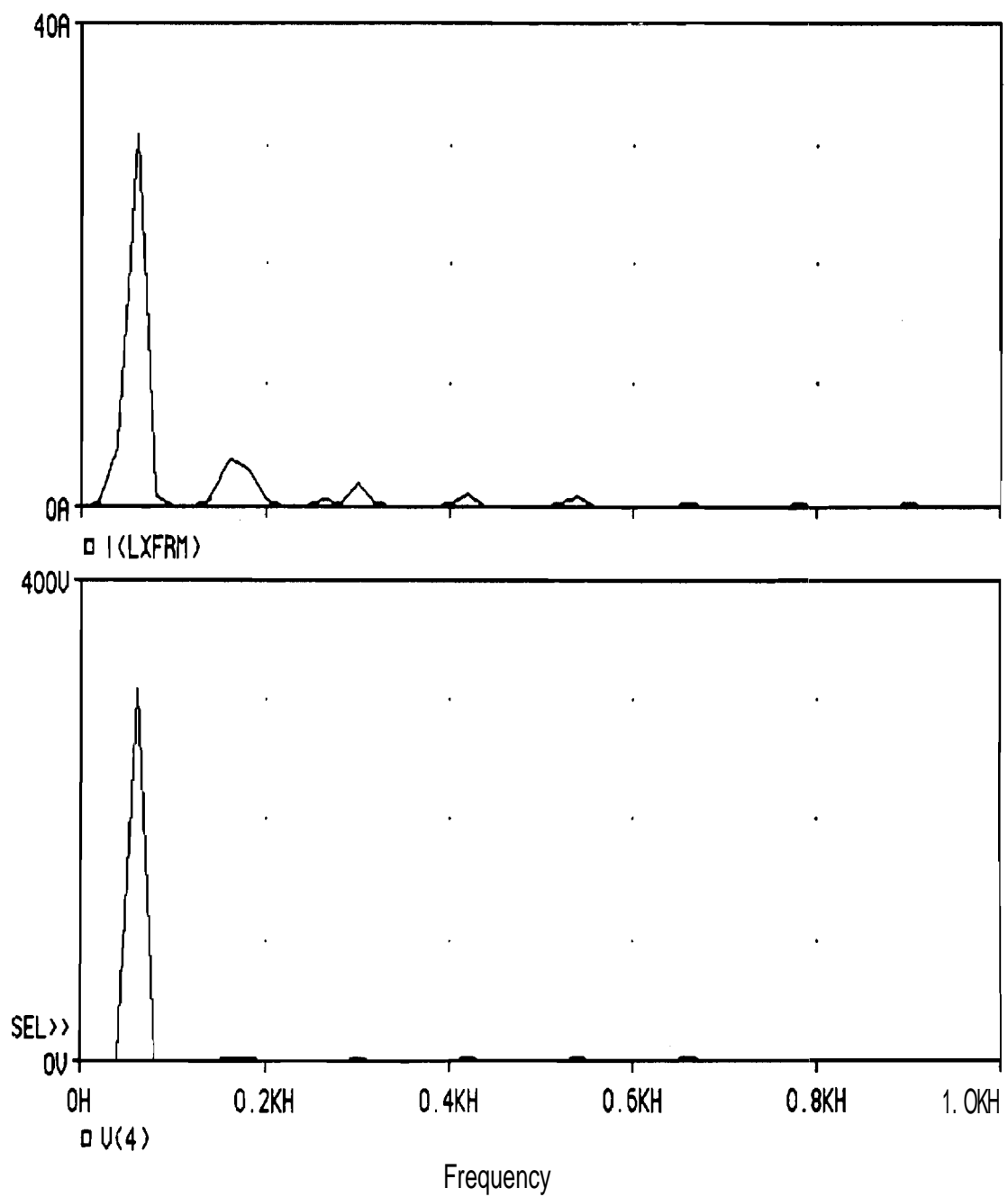


Figure 2-3d
 Secondary Current Spectrum,
 and Secondary Voltage Spectrum
 for $\alpha = 45^\circ$

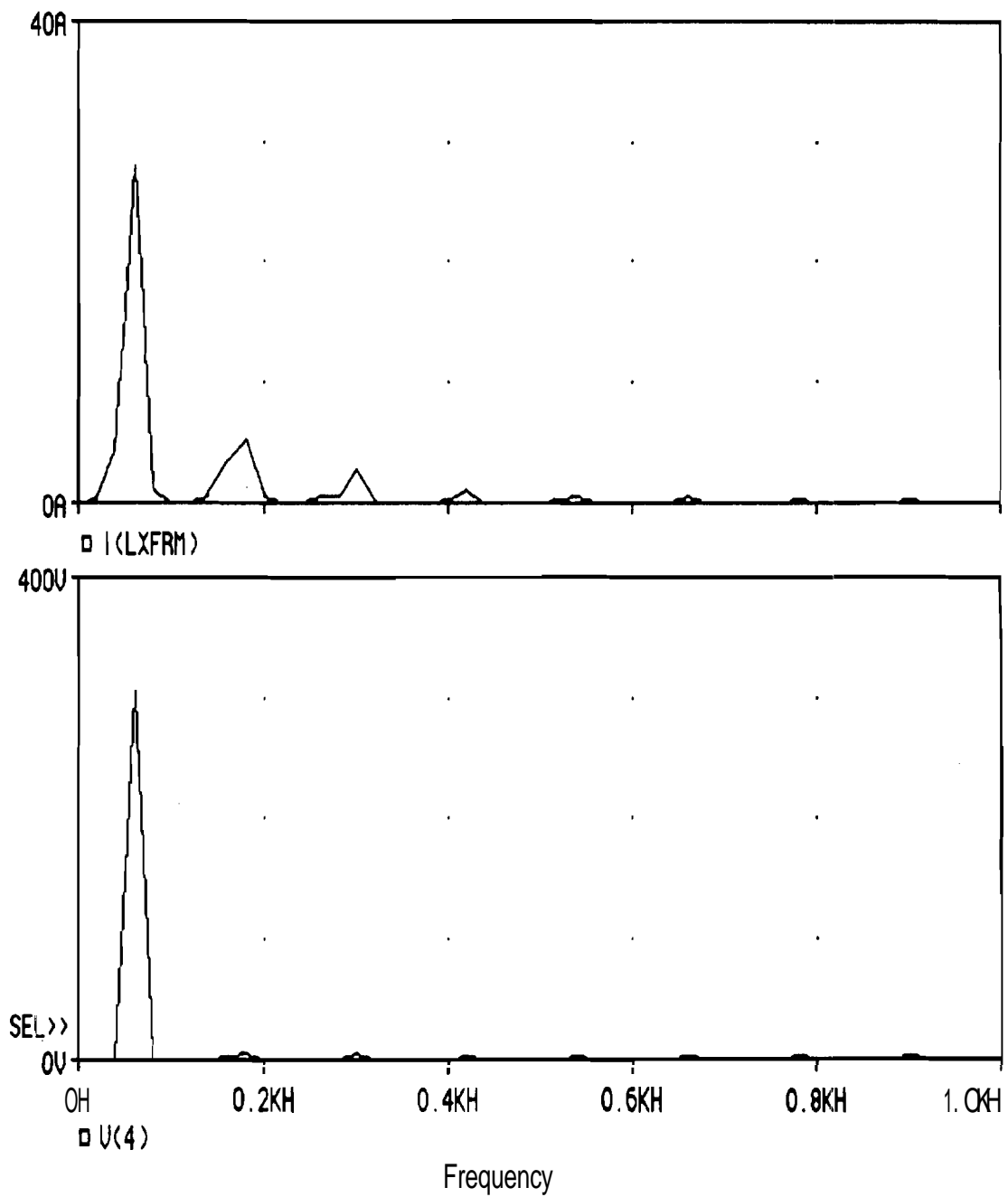


Figure 2-3e
 Secondary Current Spectrum,
 and Secondary Voltage Spectrum
 for $\alpha = 60^\circ$

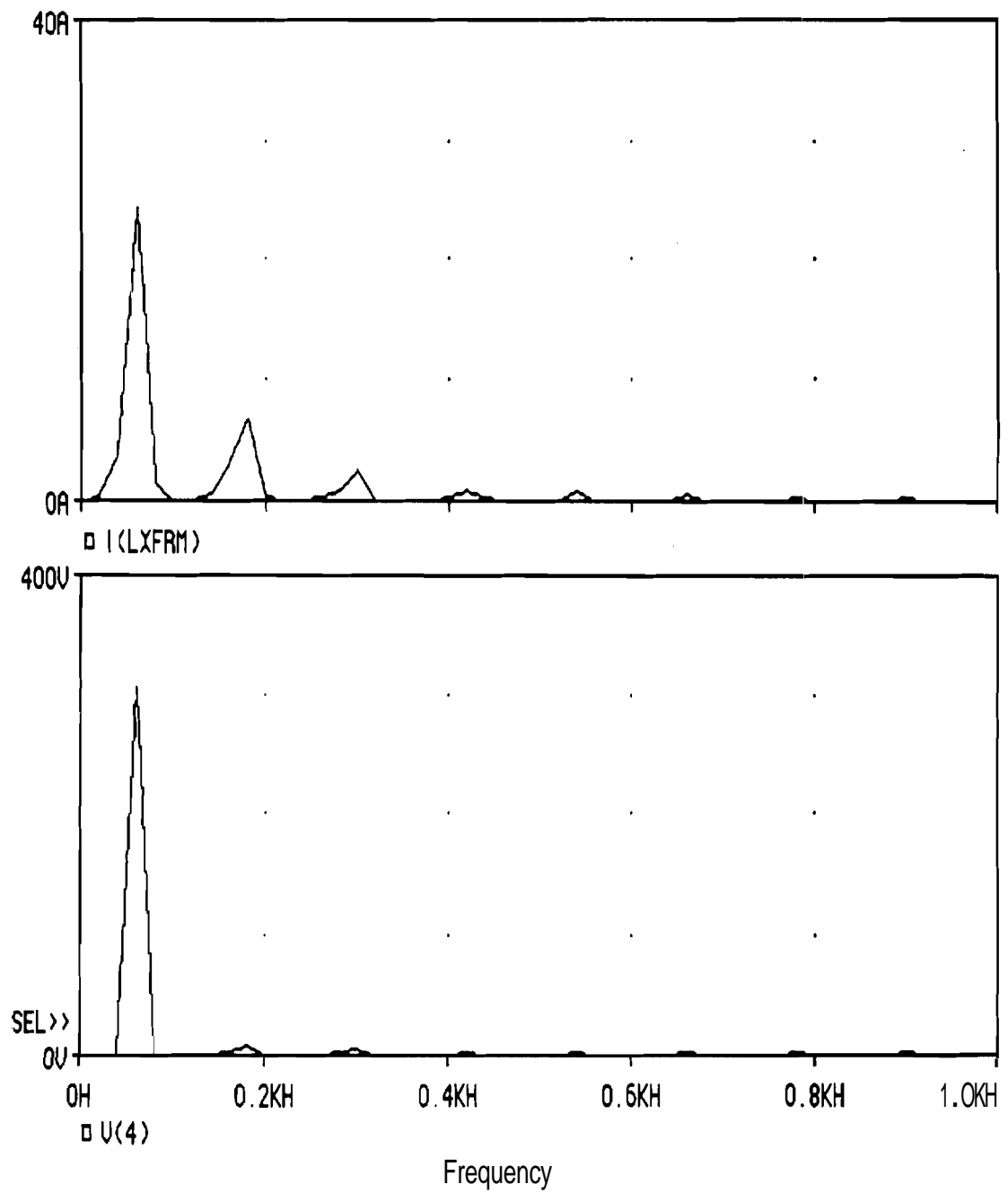


Figure 2-3f
 Secondary Current Spectrum,
 and Secondary Voltage Spectrum
 for $\alpha = 75^\circ$

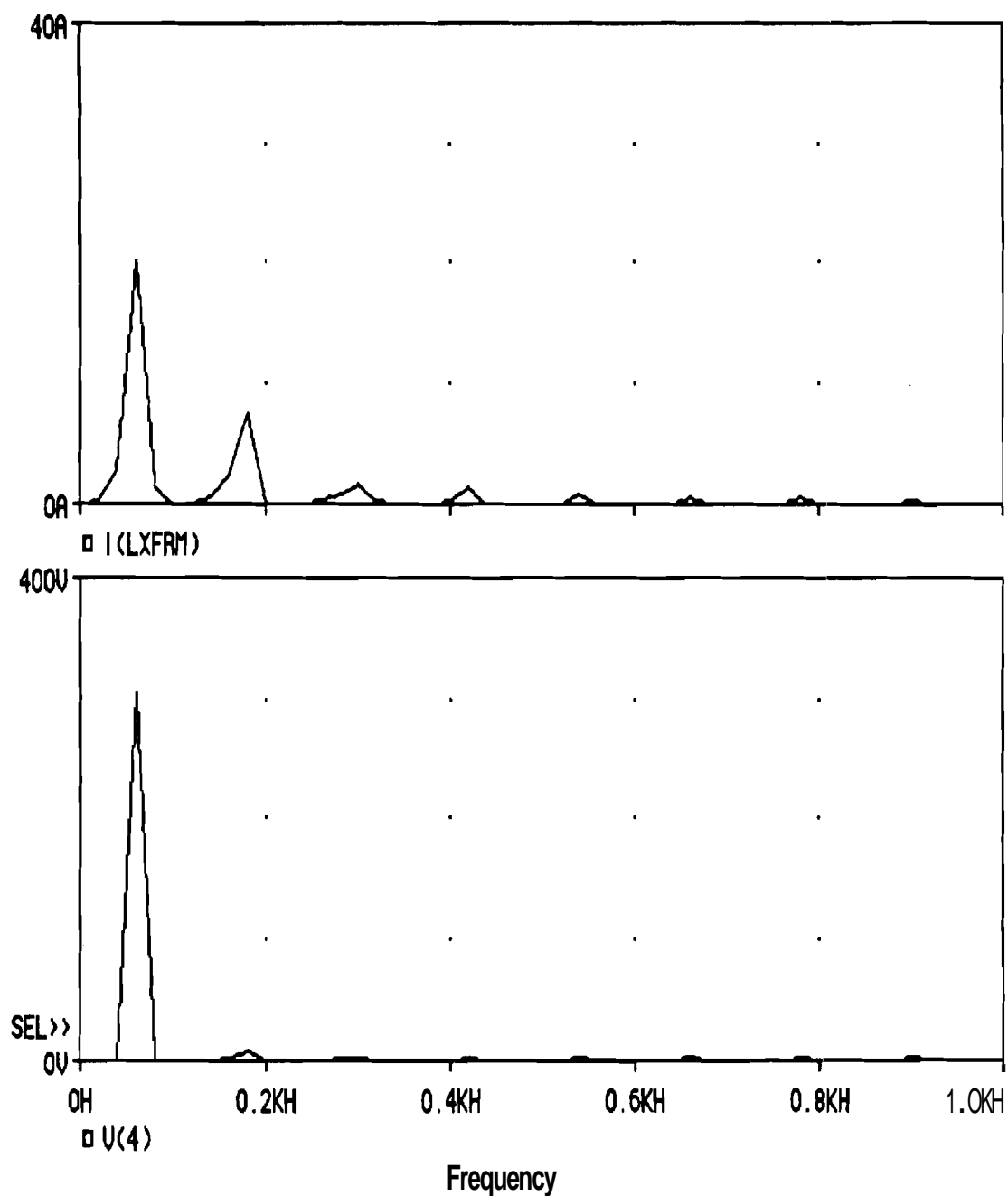


Figure 2-3g
Secondary Current Spectrum,
and Secondary Voltage Spectrum
for $\alpha = 90^\circ$

2.2 Distribution transformer derating

The harmonic distribution for the secondary current shown in Figures 2-3a through 2-3g is presented in Figure 2-4. The magnitudes of the load current for the fundamental through 15th harmonic are given. The total harmonic distortion is given by

$$\text{THD} = \frac{\sqrt{\sum_{h=2}^{15} I_h^2}}{I_1} \quad (2-2)$$

The total harmonic distortion in the load current for the various delay angles is given in Figure 2-5. Scaling the harmonic spectrum of the secondary current given in Figure 2-4 to 1 per unit leads to the harmonic spectrum of the load current in Figure 2-6.

The load current values in Figure 2-6 can be applied to Equation 1-1. Assuming the winding eddy current loss under rated conditions at the point of maximum loss density is 15% of the local 1^2R loss, all the information necessary to calculate the transformer capability is available. Using **ANSI/IEEE Recommended Practice C57.110-1986**, the transformer capability is calculated. This is shown in Figure 2.7. As an example, take the per unit load current harmonic spectrum for $\alpha = 90^\circ$ from Figure 2-6. Applying **ANSI/IEEE C57.110-1986** leads to the table on the following page.

Calculation of the transformer derating leads to the following table:

h	I_h	I_h^2	h^2	$I_h^2 h^2$	f_h	f_h^2	$f_h^2 h^2$
1	0.92939	0.86377	1	0.86377	1	1	1
3	0.35185	0.12380	9	1.11419	0.37858	0.14332	1.28992
5	0.07537	0.00568	25	0.14202	0.08110	0.00658	0.16441
7	0.06607	0.00437	49	0.21390	0.07109	0.00505	0.24763
9	0.03735	0.00140	81	0.11300	0.03696	0.00137	0.11065
11	0.02078	0.00043	121	0.05225	0.02236	0.00050	0.06049
13	0.02158	0.00047	169	0.07870	0.02322	0.00054	0.09111
15	0.01083	0.00012	225	0.02639	0.01165	0.00014	0.03055
Σ						1.15750	2.99477

Substitute the appropriate values directly into Equation 1-1. The estimate of the derating is

$$I_{MAX} = \sqrt{\frac{(1.15)}{1 + \frac{(2.99477)(0.15)}{(1.15750)}}} = 0.91021$$

or 91.0%. Thus, the transformer capability is approximately 91.0% of its sinusoidal load current capability with a delay angle α of 90°

I_h							
h	$\alpha = 0^\circ$	$\alpha = 15^\circ$	$\alpha = 30^\circ$	$\alpha = 45^\circ$	$\alpha = 60^\circ$	$\alpha = 75^\circ$	$\alpha = 90^\circ$
1	33.032	33.055	32.393	30.723	28.025	24.398	20.094
3	4.3821	4.2197	4.1761	3.9413	5.2083	6.8498	7.6072
5	0.6752	0.51582	0.82200	2.0027	2.6828	2.4525	1.6295
7	0.19755	0.06181	0.60707	1.2290	1.0992	0.80967	1.4285
9	0.0	0.0	0.45682	0.70507	0.43776	0.89427	0.80758
11	0.0	0.0	0.34729	0.36827	0.45312	0.57094	0.44917
13	0.0	0.0	0.26474	0.19050	0.41444	0.27551	0.46660
15	0.0	0.0	0.20140	0.14961	0.27577	0.30618	0.23420

Figure 2-4
Harmonic Spectrum of the Secondary Current

a	THD (%)
0°	13.4
15°	12.7
30°	13.4
45°	15.2
60°	21.4
75°	30.4
90°	39.7

Figure 2-5
Total Harmonic Distortion (THD) in the Secondary Current

$I_h(\text{pu})$							
h	$\alpha = 0^\circ$	$\alpha = 15^\circ$	$\alpha = 30^\circ$	$\alpha = 45^\circ$	$\alpha = 60^\circ$	$\alpha = 75^\circ$	$\alpha = 90^\circ$
1	0.99109	0.99183	0.99142	0.98866	0.97774	0.95687	0.92939
3	0.13148	0.12661	0.12781	0.12683	0.18171	0.26864	0.35185
5	0.02026	0.01548	0.01858	0.06444	0.09360	0.09618	0.07537
7	0.00593	0.00185	0.01858	0.03955	0.03835	0.03175	0.06607
9	0.0	0.0	0.01398	0.02269	0.01527	0.03507	0.03735
11	0.0	0.0	0.01063	0.01185	0.01581	0.02239	0.02078
13	0.0	0.0	0.00810	0.00613	0.01446	0.01081	0.02158
15	0.0	0.0	0.00616	0.00418	0.00962	0.01201	0.01083

Figure 2-6
Harmonic Spectrum of the per unit Secondary Current

a	Capability (%)
0°	99.0
15°	99.1
30°	98.7
45°	98.7
60°	96.0
75°	93.4
90°	91.0

Figure 2-6
Distribution Transformer Capability

2.3 Discussion

As the control angle α was allowed to vary from 0° to 90° , the total harmonic distortion increased as seen in Figure 2-5. This causes a slowing of the heat pump compressor which coincides with the heating/cooling demand. With this total harmonic distortion comes an associated decrease in the distribution transformer capability as shown in Figure 2-7.

In this report the change in induction motor rotor slip accompanying the change in speed of the compressor was not modeled. The slip was held constant at $1/6$. The non-ASD heat pump load was assumed constant and purely resistive. The distribution transformer was also assumed to serve only one residence. The assumption of single residence load may be appropriate for rural residences, however it is not an adequate representation for urban areas.

The fast Fourier transform as performed in PSpice was only taken over the last 60Hz period of the waveform. Thus, effects produced by the varying resistor may not appear in the fast Fourier transform of the load current or secondary voltage.

CHAPTER 3

CONCLUSIONS AND RECOMMENDATIONS

3.1 Conclusions

The use of a simple ASD heat pump model suggests a decrease in distribution transformer capability to supply load currents. This conclusion is reached on the basis that the ASD heat pump load currents are non sinusoidal. More advanced machine models are not expected to lead to a drastically different conclusion. The presence of many high efficiency heat pumps may cause a dramatic effect on the electric distribution system.

The electric utility company should reassess the costs associated with encourrrrging the use of high efficiency heat pumps. There may be hidden costs due to transformer derating and transformer losses. These costs are the consequences of non sinusoidal load currents. There may be reasons for encouraging the use of ASD heat pumps, however, the full cost of these loads should be considered. This power quality issue warrants further research.

3.2 Recommendations for future work

One extension of this report should be the inclusion of more detailed models of the electric motor and the heat pump compressor. A better model of the load torque produced by the compressor of the heat pump should be used. A more accurate model of the effect this variable load torque has on the motor should be simulated. The electronic drive used in this report is just one of several strategies

employed in obtaining variable speed. The effect that other electronic drives have upon the distribution transformer should also be examined.

ANSI/IEEE Recommended Practice C57.110-1986, as it is presently written, assumes that the non sinusoidal transformer load currents possess a Fourier spectrum with energy concentrated at integer multiples of 60Hz. Some drives do not exhibit this type of spectrum. It is recommended that the effects of load currents with other than integer harmonic spectra be examined.

Another means by which this research could be improved is the use of more accurate models of the distribution **system** for this application. This would also include a more accurate model of the distribution transformer. The impact that multiple ASD heat pumps may have on the entire electric distribution system **might** prove to be the most significant issue warranting further research in this power quality area.

LIST OF REFERENCES

- [1] G.T. Heydt, Electric Power Quality, Stars in a Circle Publications, West Lafayette, IN, 1991.
- [2] C.D. McGillem and G.R. Cooper, Continuous and Discrete Signal and System Analysis, Holt, Rinehart and Winston, New York, 1984.
- [3] H.J. Sauer, Jr. and R.H. Howell, Heat Pump Systems, John Wiley & Sons, New York, 1983.
- [4] "The Advanced Heat Pump, All the Comforts of Home...", EPRI Journal, March 1988, pp. 5-13.
- [5] S.R. Peterson, "Advanced Heat Pumps for the 1990's", ASHRAE Journal, Sep. 1989, pp. 36-46.
- [6] "Environmental Benefits of Adjustable-Speed Drive Applications", EPRI TR-100200, Research Project 2951-11, Palo Alto, CA, 1992.
- [7] M.K. Addy, "Electronic Energy Saving in Refrigeration Equipment", International Journal of Refrigeration, May 1987, pp. 175-177.
- [8] N. Mohan, T.E. Undeland, and W.P. Robbins, Power Electronics: Converters. Applications. and Design, John Wiley & Sons, New York, 1989.
- [9] G.R. Slemon, Electric Machines and Drives, Addison-Wesley Publishing Co., Inc., Reading, MA, 1992.
- [10] PSpice Circuit Analysis User's Guide, MicroSim Corp., Irvine, CA, 1991.
- [11] P.W. Tuinenga, SPICE. A Guide to Circuit Simulation & Analysis using PSpice, 2nd ed., Prentice Hall, Englewood Cliffs, NJ, 1992.
- [12] J. Alvin and P. Choi, Macromodeling with Spice, Prentice Hall, Englewood Cliffs. NJ, 1992.

- [13] "IEEE Recommended Practice for Establishing Transformer Capability when Supplying Non sinusoidal Load Currents", The Institute of Electrical and Electronics Engineers, Inc., New York, 1988.
- [14] R. Cohen, Personal conversation, Professor of Mechanical Engineering, Purdue University, 1992.

APPENDIX

PSpice Input File

heatpump.cir

```
.PARAM pulse-width = 2.0ms, slip = {1/6}, f = 60, pi = 3.14159265
*PARAM alfa = 90, icgt = 1v, iccur = 0A, period = {1/f}
```

```
VIN 1 0 sin(0V 311.127V 60 0 0 (alfa))
```

```
XSCR1 4 5 SCR params: tdly = 0, icgate = {icgt}
```

```
XSCR2 5 4 SCR params: tdly = {period*0.5},
```

```
+ icgate = {-icgt}
```

```
*XRES 7 8 TVRES
```

```
L1 8 0 6.5mH IC = {iccur}
```

```
L2 7 0 6.0H IC = {iccur}
```

```
R2 7 0 500
```

```
L3 5 6 0.65mH IC = {iccur}
```

```
R3 6 7 1.0
```

```
RLOAD 4 0 75
```

```
LXFRM 3 4 0.18mH IC = {iccur}
```

```
RXFRM 2 3 0.007
```

```
*LSYS 1 2 0.8mH IC = {iccur}
```

*

```
.SUBCKT TVRES 101 102
```

```
RSMAL 103 104 10
```

```
VSNS 104 102 0V
```

```
ERES 101 103 VALUE=
```

```
+ ( 4*I(VSENS)*sin(2*pi*2*f*(1-slip)*TIME) )
```

```
*ENDS
```

*

```
.SUBCKT SCR 101 103 params: tdly = 1ms, icgate = 0V
```

```
SW 101 102 53 0 SWITCH
```

```
VSNS 102 103 0V
```

```
RSNUB 101 104 200
```

```
*CSNWB 104 103 1uF
```

```

VGATE      5 1    0    PULSE(0 1V {tdly} 0 0 {pulse-width} {period})
RGATE      5 1    0    1MEG
EGATE      5 2    0    TABLE {I(VSENS)+V(51)} = (0.0,0.0) (0.1,1.0)
(1.0,1.0)
RSER       5 2    5 3    I
CSER       5 3    0    1uF IC = {icgate}

```

```

.MODEL SWITCH VSWITCH (RON = 0.01, ROFF = 1meg)

```

```

ENDS

```

```

*
*

```

```

.TRAN 50us 50ms 0s 50us UIC

```

```

.PROBE V(1) I(LXFRM) V(4) I(L3)

```

```

.PROBE I(L1) V(7,8)

```

```

.END

```